Atmos. Chem. Phys., 12, 12211–12225, 2012
www.atmos-chem-phys.net/12/12211/2012/
doi:10.5194/acp-12-12211-2012

Atmospheric Chemistry and Physics

Future impact of traffic emissions on atmospheric ozone and OH based on two scenarios

Ø. Hodnebrog[1,2], T. K. Berntsen[1], O. Dessens[3,*], M. Gauss[1,4], V. Grewe[5], I. S. A. Isaksen[1], B. Koffi[6], G. Myhre[2], D. Olivié[7,], M. J. Prather[8], F. Stordal[1], S. Szopa[6], Q. Tang[8,9], P. van Velthoven[10], and J. E. Williams[10]**

[1]Department of Geosciences, University of Oslo, Norway
[2]Center for International Climate and Environmental Research-Oslo (CICERO), Oslo, Norway
[3]Centre for Atmospheric Science, Department of Chemistry, Cambridge, UK
[4]Norwegian Meteorological Institute, Oslo, Norway
[5]Deutsches Zentrum für Luft- und Raumfahrt, Institut für Physik der Atmosphäre, Oberpfaffenhofen, Germany
[6]Laboratoire des Sciences du Climat et de l'Environment (LSCE-IPSL), Gif-sur-Yvette, France
[7]Centre National de Recherches Météorologiques GAME/CNRM (Météo-France, CNRS), Toulouse, France
[8]Department of Earth System Science, University of California, Irvine, USA
[9]Department of Biological and Environmental Engineering, Cornell University, Ithaca, USA
[10]Royal Netherlands Meteorological Institute, KNMI, De Bilt, The Netherlands
[*]now at: UCL Energy Institute, University College London, London, UK
[**]now at: Department of Geosciences, University of Oslo, Norway and CICERO, Oslo, Norway

Correspondence to: Ø. Hodnebrog (oivind.hodnebrog@cicero.uio.no)

Received: 2 July 2012 – Published in Atmos. Chem. Phys. Discuss.: 20 August 2012
Revised: 29 November 2012 – Accepted: 3 December 2012 – Published: 21 December 2012

Abstract. The future impact of traffic emissions on atmospheric ozone and OH has been investigated separately for the three sectors AIRcraft, maritime SHIPping and ROAD traffic. To reduce uncertainties we present results from an ensemble of six different atmospheric chemistry models, each simulating the atmospheric chemical composition in a possible high emission scenario (A1B), and with emissions from each transport sector reduced by 5 % to estimate sensitivities. Our results are compared with optimistic future emission scenarios (B1 and B1 ACARE), presented in a companion paper, and with the recent past (year 2000). Present-day activity indicates that anthropogenic emissions so far evolve closer to A1B than the B1 scenario.

As a response to expected changes in emissions, AIR and SHIP will have increased impacts on atmospheric O_3 and OH in the future while the impact of ROAD traffic will decrease substantially as a result of technological improvements. In 2050, maximum aircraft-induced O_3 occurs near 80° N in the UTLS region and could reach 9 ppbv in the zonal mean during summer. Emissions from ship traffic have their largest O_3 impact in the maritime boundary layer with a maximum of 6 ppbv over the North Atlantic Ocean during summer in 2050. The O_3 impact of road traffic emissions in the lower troposphere peaks at 3 ppbv over the Arabian Peninsula, much lower than the impact in 2000.

Radiative forcing (RF) calculations show that the net effect of AIR, SHIP and ROAD combined will change from a marginal cooling of $-0.44 \pm 13\,\mathrm{mW\,m^{-2}}$ in 2000 to a relatively strong cooling of -32 ± 9.3 (B1) or $-32 \pm 18\,\mathrm{mW\,m^{-2}}$ (A1B) in 2050, when taking into account RF due to changes in O_3, CH_4 and CH_4-induced O_3. This is caused both by the enhanced negative net RF from SHIP, which will change from $-19 \pm 5.3\,\mathrm{mW\,m^{-2}}$ in 2000 to -31 ± 4.8 (B1) or $-40 \pm 9\,\mathrm{mW\,m^{-2}}$ (A1B) in 2050, and from reduced O_3 warming from ROAD, which is likely to turn from a positive net RF of $12 \pm 8.5\,\mathrm{mW\,m^{-2}}$ in 2000 to a slightly negative net RF of -3.1 ± 2.2 (B1) or -3.1 ± 3.4 (A1B) $\mathrm{mW\,m^{-2}}$ in the middle of this century. The negative net RF from ROAD is temporary and induced by the strong decline in ROAD emissions prior to 2050, which only affects the methane cooling term due to the longer lifetime of CH_4 compared to O_3. The O_3 RF from AIR in 2050 is

strongly dependent on scenario and ranges from 19 ± 6.8 (B1 ACARE) to $61 \pm 14\,mW\,m^{-2}$ (A1B). There is also a considerable span in the net RF from AIR in 2050, ranging from -0.54 ± 4.6 (B1 ACARE) to 12 ± 11 (A1B) $mW\,m^{-2}$ compared to $6.6 \pm 2.2\,mW\,m^{-2}$ in 2000.

1 Introduction

Emissions from the transport sector have been increasing rapidly during the last decades. Larger transport demand is expected also for the future due to the growing human population and the increasing mobility. The transport sector mainly affects climate through emissions of CO_2, aerosols, water vapour, and ozone (O_3) precursors. We focus on the latter group of emissions, which is also important for air quality and the oxidative capacity of the atmosphere, and consists of the relatively short-lived gases nitrogen oxides (NO_x), carbon monoxide (CO) and non-methane hydrocarbons (NMHCs). On a 100-yr time scale, tropospheric O_3 constitutes the second largest positive radiative forcing (RF) term (after CO_2) due to present-day (year 2000) traffic emissions (Fuglestvedt et al., 2008), and one study predicts that in 2030 the traffic sector will constitute 29 % of the total anthropogenic ozone RF (Unger et al., 2008). Ozone precursor emissions also alter the levels of OH, normally leading to a reduction of methane (CH_4) lifetime and thereby a cooling of the atmosphere.

This paper follows a series of recent studies that have quantified impacts of transport emissions on atmospheric chemistry and climate (Fuglestvedt et al., 2008; Cariolle et al., 2009; Hoor et al., 2009; Skeie et al., 2009; Balkanski et al., 2010; Eyring et al., 2010; Huszar et al., 2010; Koffi et al., 2010; Lee et al., 2010; Uherek et al., 2010; Dahlmann et al., 2011; Hodnebrog et al., 2011; Myhre et al., 2011; Grewe et al., 2012; Olivié et al., 2012), and have been initiated in the framework of the EU project QUANTIFY (Quantifying the Climate Impact of Global and European Emission Systems). As in the earlier studies, the different transport sectors AIRcraft, maritime SHIPping and ROAD traffic have been studied individually. This is important because the different sectors emit various compositions of gases and particles, and at different locations, which leads to substantially different impacts on climate. More specifically, the climate impact of ROAD is dominated by warming from CO_2 while AIR is also dominated by warming from contrail cirrus formation, although the magnitude of this process is uncertain (Fuglestvedt et al., 2008; Lee et al., 2010; Burkhardt and Karcher, 2011). On the other hand, SHIP leads to a net cooling of climate due to the strong direct and indirect effect from sulphate aerosols and due to high NO_x emissions leading to a reduction of the CH_4 lifetime (Fuglestvedt et al., 2008; Balkanski et al., 2010). Current knowledge of the climate impact of transport emissions has recently been reviewed for land transport (Uherek et al., 2010), aviation (Lee et al., 2010), and shipping (Eyring et al., 2010).

Estimates of the future impact of traffic emissions on the atmospheric chemical composition depend strongly on assumptions related to the development in economy, population and technology. Here we investigate the effects on atmospheric O_3, OH, and the resulting RF in a high emission scenario for all three transport sectors, while the impacts of a low emission scenario, including a mitigation scenario for AIR, have been investigated for AIR and SHIP in a recently published companion paper (Hodnebrog et al., 2011, hereafter referred to as H2011). The emission scenarios selected for this purpose were the A1B (high), B1 (low) and B1 ACARE (mitigation) which are based on the storylines of the Special Report on Emission Scenarios (SRES) (Nakicenovic et al., 2000). Global CO_2 emissions from fossil fuel and industrial processes for 2010 are estimated to be 9.14 Gt C (Peters et al., 2012), indicating that the emission activity so far is closer to the evolution of the high A1B scenario (9.68 Gt C), which is the focus of this study (for O_3 precursors), than to the low B1 scenario (8.50 Gt C), which was studied in H2011. Due to the assumptions of a rapid decline in ROAD emissions under the B1 scenario, this sector was not investigated specifically in H2011 but has been included for the A1B scenario in this study. Until recently, the impact of ROAD on the atmospheric chemical composition has, unlike the AIR and SHIP sectors, been investigated in relatively few studies (Granier and Brasseur, 2003; Niemeier et al., 2006; Matthes et al., 2007).

Six different atmospheric chemistry models have been used to simulate changes in O_3 and OH from the three transport sectors. Section 3 presents these results along with the RF calculations. In addition, we present in Sect. 4 a synthesis of O_3 and CH_4 RF estimated from this study, H2011, and Myhre et al. (2011) to give a consistent set of results from all six models, all three transport sectors, and all scenarios, including present-day (year 2000). Such a comparison is particularly useful when considering mitigation measures, and, since a consistent set of models has been used, differences between scenarios are mostly governed by differences in emission scenarios rather than disagreements between models.

2 Methods and models

We have used gridded emission data of CO, NO_x, and NMHC (Table 1), which have been developed within QUANTIFY and can be downloaded from www.ip-quantify.eu. These data are the same as described in H2011, except that we use the A1B scenario instead of B1. The A1 storyline is much less optimistic than B1 in terms of emissions, and is characterized by very rapid economic growth, a global population that peaks in 2050, and a quick introduction of new and more efficient technologies (Nakicenovic et al., 2000).

Table 1. Global annual emissions of NO_x, CO and NMHC provided by QUANTIFY (http://www.ip-quantify.eu) for the years 2000, 2025 and 2050 in the A1B scenario. The 2000 emissions are from the final QUANTIFY dataset and thereby differ from the preliminary emissions used in Hoor et al. (2009).

	NO_x emissions in Tg(N)			CO emissions in Tg(C)			NMHC emissions in Tg(C)			
Source	2000	2025A1B	2050A1B	2000	2025A1B	2050A1B	2000	2025A1B	2050A1B	References
Aircraft	0.85	1.42	3.33	–	–	–	–	–	–	Owen et al. (2010)
Ship	4.56	6.42	8.64	0.59	1.19	2.30	0.36	0.66	1.20	Eide et al., (2007); Endresen et al. (2007)
Road	8.89	6.45	1.71	47.2	27.7	11.3	11.4	5.55	1.70	Borken et al. (2007); Uherek et al. (2010)
Non-traffic	28.9	35.7	30.1	365	485	459	108	135	119	van Aardenne et al. (2005); van der Werf et al. (2006)
Biogenic, soil	6.89	6.89	6.89	48.2	48.2	48.2	341	341	341	Jöckel et al. (2006)

Further, the A1B scenario represents a direction of technological change that is in between fossil intensive and non-fossil energy sources, i.e. assuming that similar improvement rates apply to all energy sources. For the transport sectors, these assumptions lead to a strong increase in emissions of O_3 precursors for the AIR and SHIP sectors between 2000 and 2025, and also further to 2050 (Table 1; see also Fig. 1 in H2011). On the other hand, ROAD emissions of CO, NO_x and NMHC are expected to decrease rapidly and will evolve from being the transport sector with the highest to the lowest NO_x emissions during the period from 2000 to 2050. In 2050, ROAD NO_x emissions in the A1B scenario are less than 20 % of the year 2000 emissions, due to strict vehicle emission standards and technological improvements that will outpace the steadily growing fuel consumption (Uherek et al., 2010).

Figure 1 shows the global distribution of NO_x emission changes for the three transport sectors. For the AIR sector, a relatively strong increase is expected along nearly all major flight routes between 2000 and 2025, with an even stronger increase towards 2050 when maxima can be found over Europe and Southeast Asia. This latter increase is in strong contrast to the B1 scenario when major reductions over Europe and the US are assumed (Fig. 2 in H2011). Similarly, NO_x emissions from SHIP will increase along nearly all shipping routes from 2000 to 2050 if emissions evolve according to the A1B scenario (Fig. 1). On the contrary, emissions from ROAD are expected to decline rapidly towards the middle of this century in nearly all regions except in India and China where these emissions are expected to increase between 2000 and 2025.

Six global atmospheric chemistry models have been used in this study, where five are Chemistry Transport Models (CTMs) which were driven by 6 hourly operational meteorological data from the European Centre for Medium-Range Weather Forecasts (ECMWF), and one is a Climate Chemistry Model (CCM) which was nudged towards the ECMWF data (LMDz-INCA). This provides some consistency between the various models in that the meteorological variables are identical meaning the inter-model differences shown mostly relate to either difference in the model resolution and/or chemistry rather than atmospheric transport. Model descriptions have been given in H2011 and are briefly summarized here:

1. TM4 (Williams et al., 2010) was operated by KNMI and applied at a horizontal resolution of $3° \times 2°$ and with 34 vertical layers.

2. The p-TOMCAT model (O'Connor et al., 2005) was implemented by the University of Cambridge. T21 horizontal resolution and 31 vertical layers were used for the simulations.

3. OsloCTM2 (Gauss et al., 2003a; Søvde et al., 2008) was operated by the University of Oslo and set up with both tropospheric and stratospheric chemistry, T42 horizontal resolution, and 60 vertical layers.

4. The CCM model LMDz-INCA (Hauglustaine et al., 2004; Folberth et al., 2006) was operated by LSCE with a horizontal resolution of $3.75° \times 2.5°$ and 19 vertical layers.

5. The UCI CTM (Wild et al., 2003; Hsu et al., 2005) was implemented by the University of California, and run with T42 horizontal resolution and 40 vertical layers. The model includes both tropospheric and stratospheric chemistry – the latter being calculated using a linearized ozone scheme (Linoz).

6. MOCAGE (Teyssèdre et al., 2007) was operated by Météo-France and used at a resolution of T21 horizontally, and 60 vertical layers. Both tropospheric and stratospheric chemistry were included in these simulations.

An evaluation of these models can be found in H2011 for comparisons with multi-year sonde observations of ozone annual cycles, and in Schnadt et al. (2010) for comparisons with CO aircraft measurements. The models have been run with meteorological data from year 2003 in all simulations

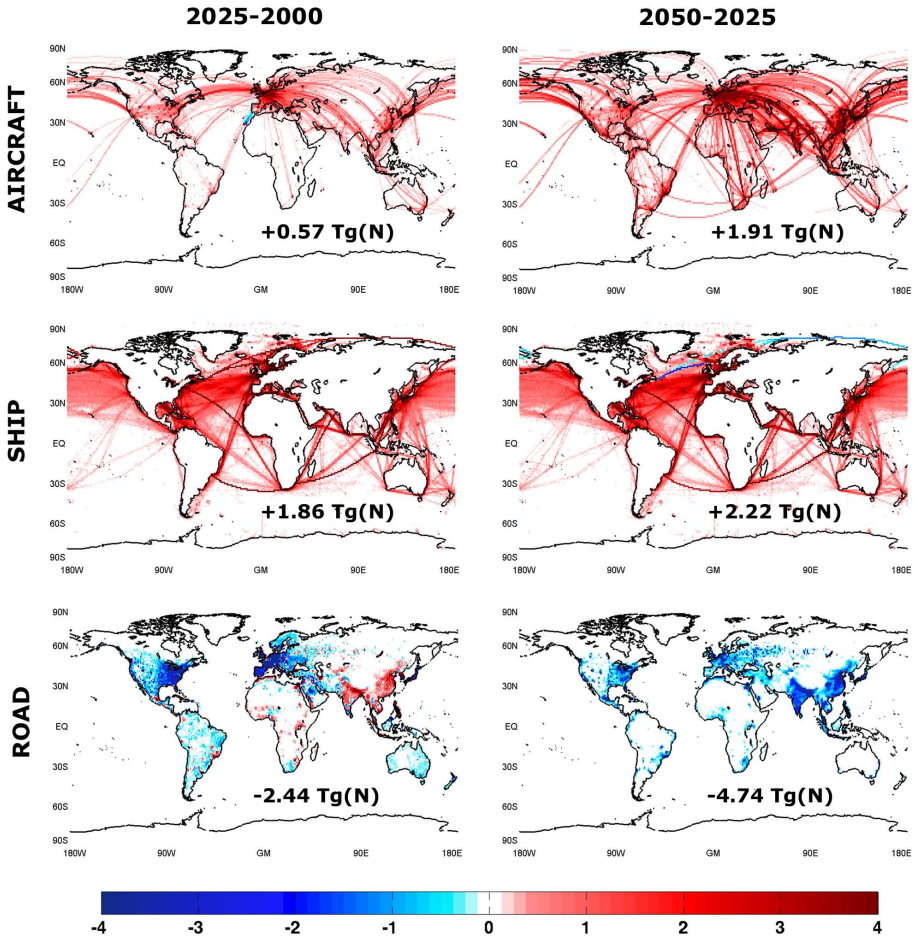

Fig. 1. Spatial distribution of the absolute difference in NO_X emission flux for the SRES A1B scenario (units: 10^{13} molecules NO_2 m^{-2} s^{-1} for AIRCRAFT and SHIP; 10^{14} molecules NO_2 m^{-2} s^{-1} for ROAD).

while 2002 was used for spin-up. For each model and each of the years 2025 and 2050, four simulations were carried out using emissions from the A1B scenario – a reference run (BASE), and perturbation runs for each of the three transport sectors AIR, SHIP, and ROAD. The reference simulation included all anthropogenic and natural emissions while in the perturbation simulations, all emitted species of the respective traffic sector were reduced by 5 % in accordance with the QUANTIFY methodology (Hoor et al., 2009; Grewe et al., 2010). It should be noted that the approach of deriving the sensitivity of the atmospheric chemical composition to each emission category by using a small perturbation has limitations in the calculation of contributions, but is suitable for addressing impacts of e.g. emission policies in the future (Grewe et al., 2010). Furthermore, Myhre et al. (2011) found that the non-linear response of a 5 % perturbation compared to a 100 % removal of the emission category is small compared to the inter-model differences in RF. This implies that the calculated sensitivities are robust, i.e. the calculated ozone change per changed mass in emissions is rather independent from the considered change in emission of either 5 % or 100 %, which is consistent with the findings in Hoor et al. (2009). The results may not be misinterpreted as contributions from the individual sectors to the ozone concentration. Grewe et al. (2012) showed that the contribution of road traffic emissions to the ozone concentration is underestimated by a factor of 5 when the contribution calculation is based on the ratio of ozone change to emission change. They showed in their simulation that the ozone chemistry is already saturated and a decrease in road traffic emissions lead to larger ozone production efficiency and larger contributions to ozone from other sectors. Hence, a large decrease in ozone contribution from road traffic is accompanied by an increase in the ozone concentrations from other sectors leading to only small changes in the ozone perturbation. For simplicity, the term "impact" is used throughout this manuscript to describe the response in O_3 and OH of a 5 % decrease in emissions from each transport sector.

It should be noted that the CTMs used here have a rather coarse grid resolution, and previous studies have shown that ozone formation may be overestimated when the emissions from e.g., aircraft and shipping are instantly diluted in a

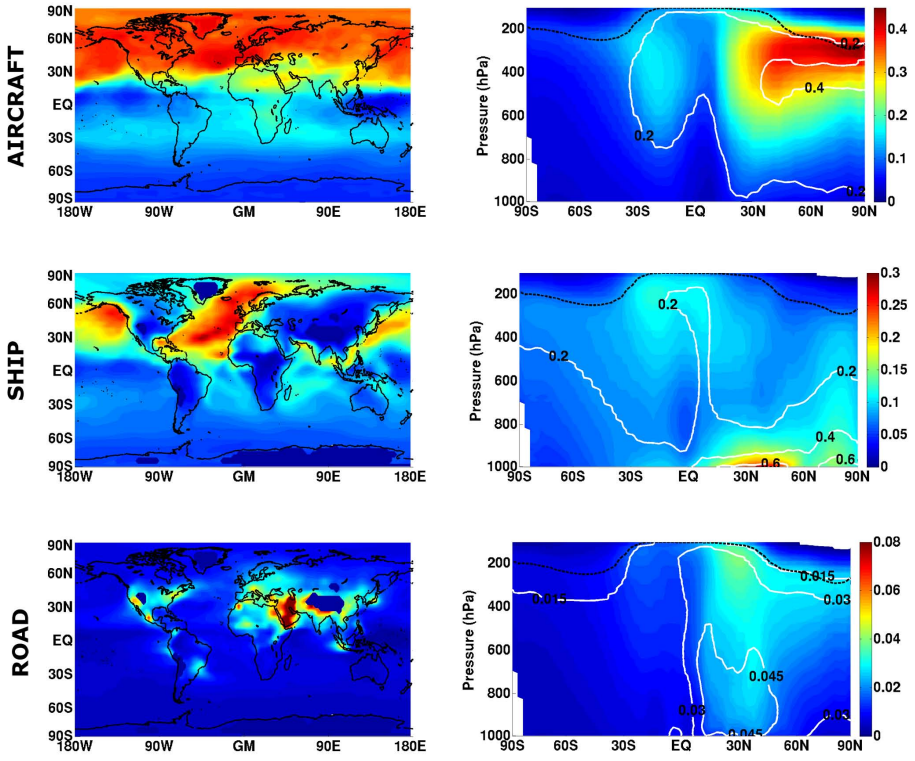

Fig. 2. Mean perturbations of ozone (ppbv) during July for the 2050 A1B scenario due to a 5 % perturbation of aircraft emissions (top), ship emissions (middle), and road traffic emissions (bottom). The left column shows ozone perturbations in the upper troposphere (300–200 hPa) for aircraft and in the lower troposphere (> 800 hPa) for ship and road traffic, while the right column shows zonal mean perturbations for each of these transport modes. In the right column, solid white contour lines show the percentage change relative to the BASE simulation while the dashed black line indicates the tropopause. Note that different scales have been used for each of the traffic sectors and that the scales have been reversed in order to show O_3 reductions, arising from a 5 % decrease in emissions, as positive numbers.

large grid box (e.g., Meijer et al., 1997; Kraabøl et al., 2002; Franke et al., 2008; Paoli et al., 2011; Vinken et al., 2011). One study suggests that ozone production due to aircraft emissions may be reduced by 10–25 % in the Northern Hemisphere when subgrid-scale plume effects are taken into account (Cariolle et al., 2009), and another study suggests a similar reduction for ship emissions – around 10–30 % over parts of the North Atlantic Ocean (Huszar et al., 2010). Although there are relatively large uncertainties related to the effects of including plume chemistry, the possible overestimation of O_3 production due to the neglect of plume processes should be kept in mind when interpreting the results presented in the subsequent sections.

Consistent with the studies of Hoor et al. (2009), Myhre et al. (2011) and H2011, the results for O_3 and OH (Sects. 3.1–3.2) are shown unscaled, i.e. the direct effect of a 5 % emission perturbation, while CH_4 lifetime changes and RF calculations (Sects. 3.3–3.4) have been scaled to 100 % by multiplying the effect of the 5 % perturbation by 20. For simplicity, we will only refer to scaled values in the text. Further details about the models and the simulation setups can be found in H2011.

3 Results and discussion – A1B scenario

3.1 Ozone

The multi-model mean impact of traffic emissions on ozone for the 2050 A1B scenario is shown in Fig. 2 for the Northern Hemisphere (NH) summer. Many features are similar to results obtained for year 2000 (Hoor et al., 2009) and the optimistic emission scenario, B1, for AIR and SHIP (H2011). Aircraft-induced O_3 is mostly confined to the NH UTLS (upper troposphere/lower stratosphere) region and is relatively well-mixed zonally, while ship emissions have their largest O_3 impact in the lower troposphere and particularly over the North Atlantic Ocean. Road traffic emissions have their maximum effects on O_3 over the Arabian Peninsula, but impacts can also be seen over urban regions in Europe, the US and South Asia which are expected to experience high increases in population by 2050. The strong impact of ROAD over Arabia is due to a combination of large emissions of O_3 precursors, inefficient O_3 dry deposition, and efficient photo dissociation, whereas the latter is caused by low zenith angles, absence of clouds, and high surface albedo which all yield high actinic fluxes of solar radiation.

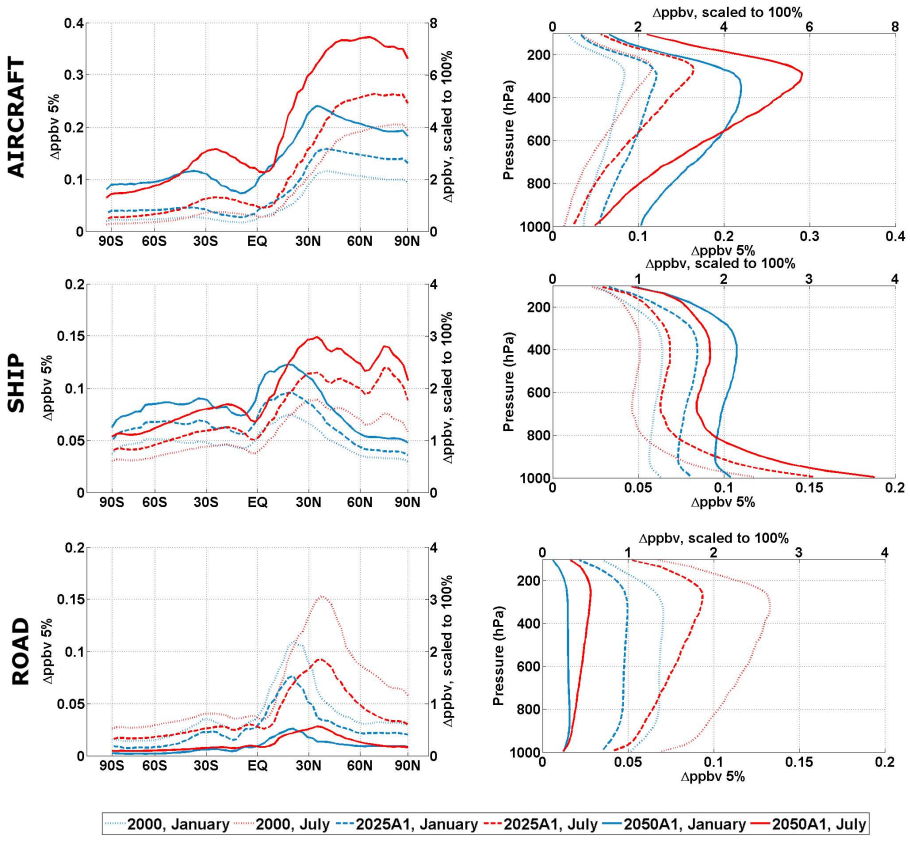

Fig. 3. Mean perturbations of ozone (ppbv) due to a 5 % perturbation of aircraft emissions (top), ship emissions (middle), and road traffic emissions (bottom). The left column shows zonally averaged ozone perturbations in the upper troposphere (300–200 hPa) for aircraft and in the lower troposphere (> 800 hPa) for ship and road traffic, while the right column shows the horizontally averaged perturbations in the Northern Hemisphere for all transport modes. The right y-axes in the left column and the top x-axes in the right column show the ozone perturbations when scaled from 5 % to 100 % by applying a factor of 20. Note that different scales have been used and that the scales have been reversed in order to show O_3 reductions, arising from a 5 % decrease in emissions, as positive numbers.

In contrast to the similarity in the global distribution of O_3 impacts, large differences can be seen regarding the magnitude of the zonal mean impacts in 2050 A1B versus 2050 B1 and 2000. While H2011 showed that zonal mean O_3 due to aircraft could reach up to 5 ppbv (ensemble mean) at northern mid- and high latitudes during summer in 2050 under the B1 scenario, the corresponding number for A1B is 9 ppbv (Fig. 2; note that the figure shows the unscaled response of a 5 % emission perturbation). The relative O_3 impact from AIR peaks in the upper troposphere and could exceed 8 % in 2050 A1B, compared to less than 4 % in 2050 B1. This large spread in O_3 impacts from AIR reflects the strong uncertainties associated with possible future developments of emissions. There are also uncertainties caused by differences between the models (e.g. different model resolution and chemistry scheme) and this is illustrated in H2011 Figs. B1–B2, which show zonal mean O_3 impacts from AIR and SHIP for each of the six models in 2050 B1. Similar inter-model differences apply for the A1B scenario presented here. The O_3 impact from SHIP differs less between the scenarios, but is still larger in A1B with a peak value over the North Atlantic Ocean of 6 ppbv (Fig. 2) compared to 4 ppbv in B1 (H2011). ROAD was not included in H2011, but comparison with the study of Hoor et al. (2009) for the year 2000 shows that the O_3 impact from this traffic sector will decrease substantially. The maximum zonal mean O_3 impact from ROAD in the lower troposphere during summer will be about 3 ppbv and the maximum zonal mean relative impact ∼ 1 % in 2050 A1B (Fig. 2), compared to more than 6 ppbv and 4 %, respectively, in year 2000 (Hoor et al., 2009).

The time evolution of transport-induced O_3 impacts since year 2000 towards 2025 and 2050 under the A1B scenario is illustrated in Fig. 3. It is evident that AIR will have the largest increase in O_3 impacts during this period, particularly between 2025 and 2050. The main reason is the assumed increase of aircraft emissions (Fig. 1), but there is also a contribution from reduced background levels of NO_x stemming from the rapid decrease of other anthropogenic emissions, particularly from road traffic, which will act to increase the O_3 enhancement efficiency of aircraft NO_x emissions. The

strong impact of ROAD on the chemical state of the UTLS in summer was highlighted in Hoor et al. (2009) and H2011. However, Table 2 shows that the effect of increased aircraft emissions will dominate the effect of reduced background NO_x levels and lead to a lower O_3 enhancement efficiency of AIR with time. The reason is that increased emissions normally leads to a smaller positive ozone perturbation per aircraft emitted NO_x-molecule due to the non-linear nature of the ozone production (e.g. Grooß et al., 1998; Grewe et al., 1999, 2012). Also worth noting for AIR is the expected increase in O_3 impacts in the Southern Hemisphere between 2000 and 2050 A1B with almost a factor of 4 difference in the zonal mean local maximum near 30° S for both seasons (Fig. 3, top left). The large increase in the NH over the same period is in strong contrast to the B1 ACARE mitigation scenario which showed a considerably lower impact on O_3 in 2050 than in 2000 (H2011).

Emissions of NO_x from SHIP are expected to increase even more than for AIR between 2000 and 2050 A1B (Fig. 1), and a corresponding increase in the ship-induced O_3 impact can be seen at all latitudes and altitudes for both seasons (Fig. 3, middle row). However, the absolute increase in O_3 mixing ratio due to SHIP in the planetary boundary layer (PBL) is much lower than that due to AIR in the UTLS. The reason is that near the surface where the SHIP emissions take place, reservoir species of NO_x, such as HNO_3 and PAN, are more rapidly removed by wet scavenging and dry deposition than in the UTLS (Hoor et al., 2009). In addition, model results show that concentrations of HO_2 increase with decreasing altitude, leading to a shorter lifetime of ozone produced near the surface. This is also reflected in the much lower O_3 enhancement efficiency for SHIP than for AIR (Table 2). Similar to AIR, the O_3 enhancement efficiency is reduced with time as a response to the increased emissions from anthropogenic sources in total. An interesting point regarding seasonal variations is the much higher sensitivity of O_3 mixing ratios in the lower troposphere to changes in ship emissions, and corresponding lower sensitivity of O_3 mixing ratios in the upper troposphere, in the NH during summer compared to winter (Fig. 3, middle right). All models show this signal, indicating that it is a robust feature. Near the surface there is almost a factor of 2 difference in the ensemble mean between January and July (for all years), and this is caused by the more stable maritime boundary layer and thereby less efficient vertical transport during summer.

As mentioned previously, the O_3 impact due to ROAD will be reduced dramatically in the future as a consequence of the expected decline in O_3 precursor emissions for this transport sector. In the PBL zonal mean for NH summer, the O_3 impact from ROAD peaks near 40° N with a value exceeding 3 ppbv in 2000, while the corresponding number is only 0.5 ppbv in 2050 A1B (Fig. 3, bottom left). Due to the more polluted continental boundary layer, where ROAD emissions take place, the O_3 enhancement efficiency for this traffic sector is the lowest when comparing with SHIP and AIR (Table 2). It is also the only traffic sector which has a higher O_3 enhancement efficiency in 2050 A1B than in 2000, reflecting the decrease in NO_x emissions from ROAD.

Table 2. Global annual average of the change in O_3 molecules per NO_x molecule emitted from the different transport sectors, given as ensemble means and standard deviations.

	AIR	SHIP	ROAD
2000	2.05 (± 0.51)	0.509 (± 0.19)	0.329 (± 0.11)
2025A1B	1.90 (± 0.44)	0.465 (± 0.18)	0.323 (± 0.10)
2050A1B	1.65 (± 0.27)	0.460 (± 0.19)	0.369 (± 0.13)

3.2 Global OH

Figure 4 shows the zonal mean perturbations of the hydroxyl radical (OH) in 2050 A1B for 5 % perturbations of each of the three transport sectors. In the troposphere, OH is the main oxidant and changes in its concentrations are particularly relevant for this study through the reaction with CH_4 and subsequent consequences for the radiative forcing budget. Due to the short OH lifetime of less than one second, the global distribution of transport-induced OH (Fig. 4) reflects the locations of emissions, but is also strongly affected by incoming solar radiation, the amount of water vapour, the levels of background pollution, and the lifetime of the emitted species. Furthermore, the ratio of CO to NO_x emissions differs largely between the three transport sectors. ROAD has the largest ratio and thereby lowest OH enhancement efficiency, while AIR and SHIP have low CO/NO_x ratios and are efficient in perturbing OH.

The impact of AIR on OH concentrations in northern summer 2050 A1B peaks south of the North Atlantic flight corridor (where the humidity is larger and solar zenith angle lower than further north) with a value of 3×10^5 molecules cm^{-3} (Fig. 4), which is almost twice the value predicted for the same year under the B1 scenario (H2011). In year 2000, SHIP was the transport sector which had the largest impact on the global OH budget due to large amounts of NO_x which were released into the relatively clean maritime boundary layer (Hoor et al., 2009). Our results indicate that the OH impact from SHIP is even stronger in 2050 A1B and with absolute values that peak near the surface at northern midlatitudes (Fig. 4, middle). As was the case with ozone, the impact of ROAD on global OH concentrations is expected to decrease markedly from 2000 to 2050. While Hoor et al. (2009) showed that road traffic emissions led to a maximum zonal mean increase of 1×10^5 molecules cm^{-3} near 800 hPa and 40° N in 2000, the corresponding value is only 2.5×10^4 molecules cm^{-3} in 2050 A1B (Fig. 4, bottom).

Table 3. Relative changes (%) in methane lifetime (integrated up to 50 hPa) due to a 5 % decrease in traffic emissions. Values are global annual averages given relative to the BASE simulation, and are scaled to 100 % by multiplying with 20. Both the mean of the six models and the standard deviations (indicating the spread of the models) are given. Note that this table does not include the feedback effect of methane changes on its own lifetime.

	AIR	SHIP	ROAD
2000	1.30 (± 0.30)	3.68 (± 0.47)	1.44 (± 0.81)
2025A1B	1.91 (± 0.46)	4.44 (± 0.39)	1.21 (± 0.61)
2050A1B	4.08 (± 0.83)	5.32 (± 0.56)	0.331 (± 0.11)

3.3 Methane lifetime

Relative changes in methane lifetime due to reaction with OH are presented in Table 3 (see Table A1 for results from individual models) for perturbations in each transport sector and each year. Monthly mean CH_4 and OH fields were used for the calculation, and the resulting lifetime changes were scaled from a 5 % perturbation to a 100 % perturbation by multiplying with a factor of 20 (Grewe et al., 2010). For reference, the model mean and standard deviation of the methane lifetime in the BASE simulation is 8.4 (± 1.1) yr for 2050 A1B compared to 8.3 (± 1.0) yr in 2000.

The sensitivity of OH to traffic emissions is largest in regions where the amounts of sunlight and water vapour are high, and the background concentrations of ozone, NO_x and NMHCs are low. As discussed in Hoor et al. (2009) this leads to the largest changes in methane lifetime for SHIP, which emits mainly in the relatively pristine tropical and subtropical oceans, while the impact of ROAD on methane lifetime changes is much lower since these emissions take place at higher latitudes and they can be rapidly transported aloft over the continents. Additionally, ROAD emissions have a much higher CO to NO_x ratio and are also more affected by other anthropogenic pollution sources. Considering the much lower NO_x emissions from AIR compared to ROAD and SHIP in year 2000 (Table 1), the efficiency in perturbing methane lifetime is relatively large also for this sector (Table 3).

In the future, changes in methane lifetime changes largely reflect the evolution of emissions for the various transport sectors. AIR will have the largest increase, from 1.3 to 4.1 % between 2000 and 2050 A1B, and SHIP remains the sector with the largest impact on methane lifetime, with a 5.3 % perturbation in 2050 (Table 3). It is likely that regional changes in the distribution of emissions contribute to these enhancements since both AIR and SHIP show particularly large emission increases at lower latitudes (Fig. 1), where solar radiation is stronger and water vapour levels are higher. For ROAD, however, the large reduction in road traffic-induced OH concentrations, discussed in Sect. 3.2, causes this traffic sector to induce only minor changes in methane lifetime

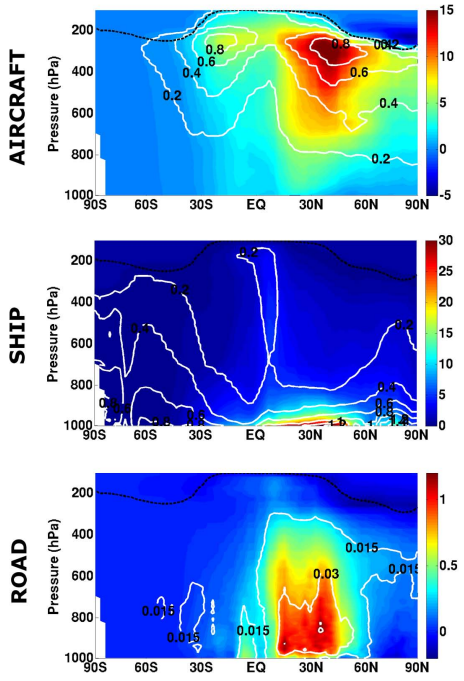

Fig. 4. Zonal mean perturbations of OH (10^3 molecule cm^{-3}) during July for the 2050 A1B scenario due to a 5 % perturbation of aircraft emissions (top), ship emissions (middle), and road traffic emissions (bottom). Solid white contour lines show the percentage change relative to the BASE simulation while the dashed black line indicates the tropopause. Note that different scales have been used for each of the traffic sectors and that the scales have been reversed in order to show OH reductions, arising from a 5 % decrease in emissions, as positive numbers.

(0.33 %) in 2050 (Table 3). When comparing with the low emission scenario B1, we see that changes in methane lifetime may evolve in very different paths, most notably for AIR which will cause a change of only 1.7 % in 2050 B1 and only 1.2 % under the B1 ACARE mitigation scenario (H2011).

3.4 Radiative forcing

We have used the Oslo radiative transfer model (Myhre et al., 2000) to calculate cloudy-sky O_3 radiative forcings with stratospheric temperature adjustment included. Monthly mean ozone fields from each of the six models were used for the calculations. An interesting finding is that the use of a scaling approach, where the global average transport-induced O_3 column were multiplied with the normalized radiative forcing (NRF; RF divided by the change in O_3 column expressed in Dobson Units (DU)), introduced only minor changes in the results compared to carrying out complete radiative transfer calculations. However, as the NRFs are dependent on both the region and altitude of the resulting O_3 change (Berntsen et al., 2000; Gauss et al., 2003b) it is important to use separate NRFs for each traffic sector due to the different locations of emissions from each sector. When using

NRFs for each traffic sector and for each of the six models based on the results from Myhre et al. (2011) (year 2000) and H2011 (years 2025/2050 and scenarios B1/B1 ACARE), the estimated O_3 RF for the A1B scenario were in most cases less than 5 % different from the results of the detailed RF calculations.

The resulting global average transport-induced O_3 RF is presented in Table 4 (see Table A2 for individual model results). In the future, AIR will be the transport sector with the largest O_3 RF, and this forcing term will more than double between 2025 and 2050, if the emissions evolve according to the A1B scenario. The O_3 RF from SHIP will also increase over the same period, while ROAD will evolve from being the transport sector with the largest O_3 radiative forcing in year 2000 (Myhre et al., 2011) to only represent 6 % of the total transport-induced O_3 RF in 2050 A1B. Further discussion of short-term O_3 RF and comparisons with other studies are given in Sect. 4.

Table 4 also gives the radiative forcings due to changes in CH_4 and subsequent changes in O_3 (long-term effect). Normally, emissions of NO_x from the transport sectors lead to increased OH concentrations and thereby reductions of CH_4 lifetime and concentrations. The second CH_4 RF term is known as the primary mode and represents the negative long-term effect of the methane perturbation on O_3 (e.g. Wild and Prather, 2000; Wild et al., 2001). The method of calculating CH_4 RF is described in Berntsen et al. (2005) and consists of first multiplying the changes in methane lifetime (presented in Table 3) with the estimated CH_4 concentrations from IPCC (2001). A feedback factor of 1.4 was used to take into account the impact of CH_4 changes on its own lifetime (IPCC, 2001). Next, linearized CH_4 specific forcings of 0.33 and $0.31\,\mathrm{mW\,m^{-2}\,ppbv^{-1}}$ were applied, assuming background CH_4 mixing ratios of 2114 and 2400 ppbv for 2025 and 2050 A1B, respectively. Finally, we have taken into account the impact of CH_4 changes on stratospheric water vapour (SWV) by assuming that the RF of SWV is a factor 0.15 times the RF of CH_4 (Myhre et al., 2007).

To calculate the RF from changes in CH_4-induced O_3 we have assumed a 0.64 DU increase in O_3 from a CH_4 increase of 10 % (for a system which has reached a new steady state) (Berntsen et al., 2005), and a specific forcing of O_3 of $42\,\mathrm{mW\,m^{-2}\,DU^{-1}}$ (IPCC, 2001). Also, to correct for the transient response, i.e. that the CH_4 concentration may not be in steady state with the OH change during the simulation year, we have applied factors based on the method described in Grewe and Stenke (2008). For the A1B scenario in 2025/2050, these factors are 0.77/0.74 for AIR, 0.85/0.88 for SHIP, and 1.07/1.77 for ROAD. The factors for ROAD are larger than 1 because of the decline in emissions from this transport sector in the years prior to the simulation year.

As for O_3 RF, the RF due to CH_4 and CH_4-induced O_3 will be stronger for AIR and SHIP, and weaker for ROAD in the period from 2025 to 2050 (Table 4). The resulting net RF shows that the positive O_3 term will dominate for AIR in the future, and will also strengthen between 2025 and 2050. For SHIP, the cooling terms of RF due to CH_4 and CH_4-induced O_3 changes will dominate and also strengthen over the same period. ROAD yielded the largest positive net RF of the three transport sectors in 2000 (Myhre et al., 2011), but will in 2050 shift from a net positive to a net negative forcing. The reason is the strong decline in ROAD emissions, which leads to a high factor to correct for the transient response (1.77 as noted above). As the short-term O_3 RF is not influenced by the time-history of emissions, the cooling effect will compensate the warming effect and lead to a net negative RF. It should be noted here that although all six models yield a negative net RF for ROAD in 2050 A1B, the relatively large standard deviation indicates that the magnitude and even the sign of the net forcing is uncertain.

4 Synthesis of RF in various scenarios

We present here a synthesis of transport-induced RF in various scenarios based on results from the same set of atmospheric chemistry models, each using the same setup and emissions data. The models and setup have been described in Myhre et al. (2011), H2011, and Sect. 2 in this paper, while the method for RF calculations used to complement the results presented in previous literature has been described in Sect. 3.4. The results from H2011 have been kept unchanged, while we have added results from the MOCAGE model to the year 2000 data presented in Myhre et al. (2011), although this only introduces minor differences. The results for the B1 scenario presented in H2011 did not include ROAD, but these results have been added here based on new radiative transfer calculations. The factors to correct for the transient response in the calculation of RF due to CH_4 for ROAD in the B1 scenario are 1.56 and 2.57 for 2025 and 2050, respectively.

Figure 5 shows the resulting RF from the six models (ensemble mean and standard deviation) for each of the three transport sectors. Focusing on RF due to O_3 (Fig. 5, top), there is clearly a large uncertainty in the magnitude of impact from AIR in the middle of this century. Although there is a considerable spread between the models (see Holmes et al. (2011) for a discussion of RF uncertainties when modelling aviation NO_x), the uncertainty is mostly induced by the large spread of emissions between the various scenarios (Lee et al., 2010), whereas the ensemble mean O_3 RF is 61 ($\pm$ 14) $\mathrm{mW\,m^{-2}}$ for the A1B scenario and only 19 ($\pm$ 6.8) $\mathrm{mW\,m^{-2}}$ for B1 ACARE in 2050, just slightly higher than in 2000 ($18 \pm 3.6\,\mathrm{mW\,m^{-2}}$). However, it should be noted here that B1 ACARE is a mitigation scenario assuming extensive technological improvements to the aircraft and is considered very optimistic in terms of emissions (see H2011). For comparison, Skeie et al. (2009) used the same set of emissions data for the A1B and B1 scenarios to yield RF due to O_3 of 82 and $38\,\mathrm{mW\,m^{-2}}$, respectively, significantly higher than our forcing results. The main reasons

Table 4. Radiative forcings (mW m^{-2}) from changes in ozone, methane (including stratospheric water vapour), and methane-induced ozone ($O_{3(CH_4)}$) for different transport sectors and years given as ensemble means and standard deviations. Note that the history of emissions has been taken into account (see text for details), and that the fully scaled perturbations were used.

		AIR				SHIP				ROAD			
		O_3	CH_4	$O_{3(CH_4)}$	total	O_3	CH_4	$O_{3(CH_4)}$	total	O_3	CH_4	$O_{3(CH_4)}$	total
2025A1B	mean	30.2	−16.7	−6.10	7.36	27.8	−42.7	−15.6	−30.5	21.4	−14.6	−5.35	1.40
	σ	10	4.0	1.5	7.3	10	3.8	1.4	8.4	5.6	7.4	2.7	8.6
2050A1B	mean	61.3	−36.4	−13.3	11.6	36.9	−56.6	−20.7	−40.4	6.48	−7.04	−2.57	−3.13
	σ	14	7.4	2.7	11	14	6.0	2.2	9.5	2.1	2.4	0.89	3.4

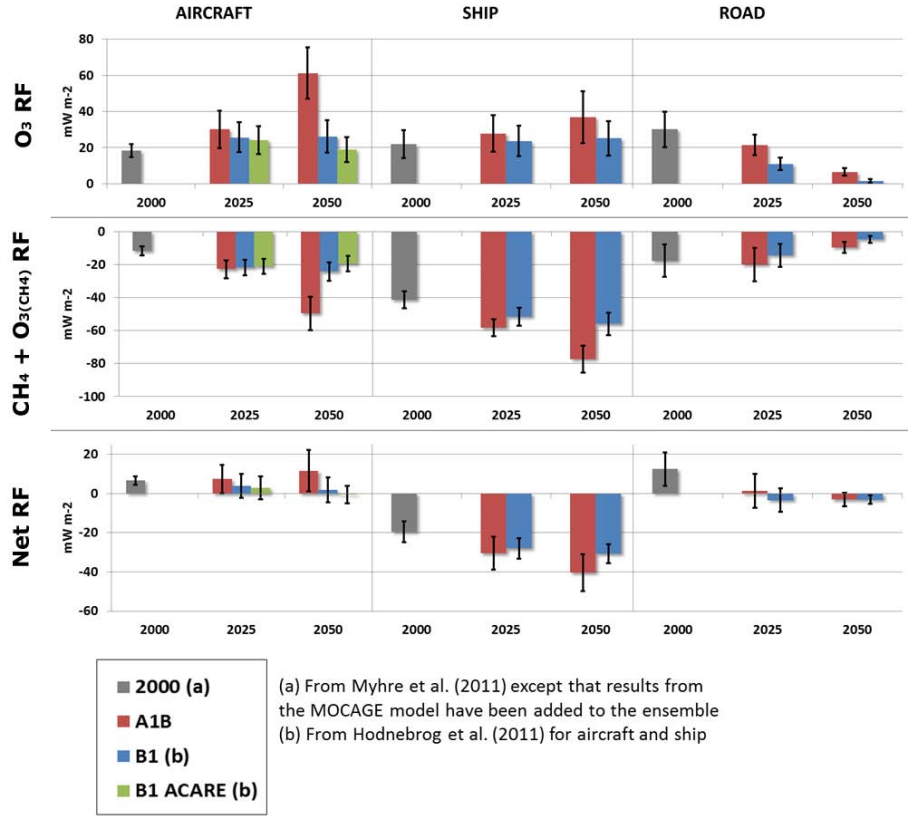

Fig. 5. Global and annual mean RF (mW m^{-2}) due to changes in short-term O_3 (top row), CH_4 including CH_4-induced O_3 (middle row) and the net RF (bottom row) as mean (coloured bars) and standard deviation (error bars) of the six models in the ensemble. Note that the time-history of emissions and the stratospheric water vapour effect have been taken into account.

are that higher NRFs (18–19 % higher) and ozone enhancement efficiencies (25–63 % higher) were used in their study. The scaling approach of Lee et al. (2009) yielded even higher aircraft-induced O_3 RF for 2050, with a range 59–110 mW m^{-2}, but the NO_x emissions used in that study were also higher.

The emission scenarios show a smaller spread for SHIP, and therefore the differences in the future O_3 RF due to shipping are also smaller (Fig. 5, top). In 2050, the O_3 RF due to shipping is estimated to be in the range from 25 ($\pm$ 9.6) to 37 ($\pm$ 14) mW m^{-2}, depending on the scenario, compared to 22 ($\pm$ 7.7) mW m^{-2} in 2000. Skeie et al. (2009) calculated substantially stronger impacts for 2050 with the range 36–62 mW m^{-2}, again due to the higher O_3 enhancement efficiencies (61–87 % higher) used in their study. Estimates from the multi-model study of Eyring et al. (2007) were much lower than in this study with O_3 RF from SHIP of 14 mW m^{-2} for 2030, and 9.8 mW m^{-2} for 2000. Part of the reason is the magnitude of ship NO_x emissions which was lower in their study, but it can also be related to the different geographical emission distribution, whereas the emission inventory used in Eyring et al. (2007) is more concentrated

along major shipping routes compared to the QUANTIFY emissions which are more widespread. Due to the non-linear nature of the ozone chemistry, this could lead to very different ozone enhancement efficiencies and subsequent discrepancies in the forcings. Contrary to AIR and SHIP, the impact of ROAD emissions on ozone RF is expected to decline rapidly in the future and yield values in the range from 1.6 ($\pm$0.91) to 6.5 ($\pm$2.1) mW m^{-2} in 2050 (Fig. 5, top). The decreased impact of ROAD in 2050 compared to 2000 is a consequence of the assumed reduction of NO_x emissions, and is also consistent with the results of Skeie et al. (2009).

When also taking into account the CH_4 RF and CH_4-induced O_3 RF, the net impact of positive and negative RF terms for AIR nearly cancel out for the two most optimistic emission scenarios (B1 and B1 ACARE) in 2050, and even yield a slightly negative net impact for the mitigation scenario (Fig. 5, bottom). On the other hand, the highest emission scenario (A1B) yields net RF due to AIR of 12 ($\pm$ 11) mW m^{-2}, almost twice the impact in 2000. For SHIP, the impact on net RF is negative in 2000, and its absolute impact will increase in the future for both the A1B and B1 scenarios. ROAD had the largest positive impact on net RF in 2000, but it will probably shift to yield slightly negative net impact in 2050 for both scenarios. As mentioned in Section 3.4, the net negative impact is present because we take into account the time-history of emissions, which in this case gives additional weight to the long-lived cooling terms (CH_4 RF and CH_4-induced O_3 RF) due to the rapid decline of NO_x emissions for ROAD in the years preceding 2050. It is also worth noting the net RF due to changes in O_3 and CH_4 from all three transport sectors combined, which is slightly negative in 2000 (-0.44 ± 13 mW m^{-2}), and strongly negative in 2050 (-32 ± 18 mW m^{-2} for A1B and -32 ± 9.3 mW m^{-2} for B1), partly due to the reduced impact of ROAD. In order to assess the total climate impact from the transport sectors, RF due to changes in e.g. CO_2, SO_2 and BC must be included and will yield very different net forcings (see e.g. Olivié et al., 2012).

5 Conclusions

The future impact of traffic emissions on atmospheric ozone and OH has been studied and quantified using six atmospheric chemistry models. The purpose of this paper is twofold. First, new results were presented for a scenario representing a possible high development of emissions (SRES A1B). Second, the radiative forcing results calculated for A1B were put in a larger context by comparing with recent literature presenting impacts of traffic emissions in possible low emission scenarios (B1 and B1 ACARE) and also for year 2000.

We find that the impacts of the non-land based traffic sectors (AIR and SHIP) on atmospheric O_3 will increase substantially in the future if emissions evolve according to the A1B scenario. Maximum impacts of O_3 due to AIR occur in the UTLS region and could reach 9 ppbv (monthly and zonally averaged) at high northern latitudes during summer in 2050, while SHIP peaks over the North Atlantic Ocean with a maximum value of 6 ppbv in the PBL during NH summer in 2050. On the contrary, ROAD will have a considerably lower impact on atmospheric O_3 in the future, due to assumptions of improvements in the NO_x technology which will outpace the increased demand. In accordance with the evolution of emissions in the A1B scenario, ozone enhancement efficiencies will increase for ROAD and decrease for AIR and SHIP.

In 2050, SHIP remains as the sector with the largest impact on global OH concentrations, and consequently yields the greatest relative change in CH_4 lifetime with 5.3 %. The largest change in the CH_4 lifetime reduction between 2000 and 2050 is for AIR which will induce a 4.1 % shorter lifetime in the middle of the 21st century. Part of the increase for AIR and SHIP is presumably caused by regional changes in the emission distributions, with large increases at low latitudes, which favours enhancements of OH concentrations. As for O_3, ROAD will have a reduced impact on atmospheric OH in the future, and cause a relative change in CH_4 lifetime of only 0.33 % in 2050.

Radiative forcing calculations, taking into account changes in O_3, CH_4 and CH_4-induced O_3, show that the future impact of AIR will increase for all RF terms, but that the magnitude of change is largely dependent on the emission scenario with a net RF ranging from -0.54 ± 4.6 (B1 ACARE) to 12 ± 11 mW m^{-2} (A1B) in 2050. SHIP will also increase its impact for all RF terms in the future, but the increase for the cooling terms (CH_4 and CH_4-induced O_3) will dominate to yield a stronger net negative RF in the future, namely between -40 ± 9.5 (A1B) and -31 ± 4.8 mW m^{-2} (B1) in the middle of this century. Comparison with previous literature reveals large spread in the magnitude of present-day and future ship-induced impact on O_3 RF, and suggests that this issue should be given increased attention, especially considering the assumed future increase of SHIP emissions. ROAD will evolve from having the largest impact on O_3 RF and the largest positive impact on net RF among the transport sectors in 2000, to having only a modest impact on O_3 and a net RF that is likely to shift to slightly negative in 2050 (net RF of -3.1 ± 3.4 (A1B) and -3.1 ± 2.2 mW m^{-2} (B1)).

The sum of net RF, taking into account O_3 and CH_4 effects, from all three transport sectors shows that there will be a shift from slightly negative net RF in 2000 (-0.44 ± 13 mW m^{-2}) to strong negative net RF in 2050 (of -32 ± 9.3 (B1) and -32 ± 18 mW m^{-2} (A1B)), mainly due to the combined impact of enhanced cooling from SHIP and reduced warming from ROAD. However, the total climate effect of future transport emissions, also taking into account the RF terms from aerosols and long-lived greenhouse gases, is largely positive and dominated by warming due to CO_2 emissions from road traffic (Olivié et al., 2012).

Appendix A

Results from individual models

Results from each of the six models are given for relative changes in CH_4 lifetime in Table A1, and for RF calculations in Table A2.

Table A1. Relative changes (%) in methane lifetime (integrated up to 50 hPa) due to a 5 % decrease in traffic emissions. Values are global annual averages given relative to the BASE simulation, and are scaled to 100 % by multiplying with 20. Note that this table does not include the feedback effect of methane changes on its own lifetime.

	TM4	p-TOMCAT	OsloCTM2	LMDz-INCA	UCI CTM	MOCAGE
AIR 2000	1.27	1.61	0.852	1.07	1.60	1.41
AIR 2025A1B	2.03	2.44	1.20	1.54	2.10	2.18
AIR 2050A1B	4.57	4.58	2.68	3.43	4.65	4.58
SHIP 2000	4.17	3.44	3.77	3.20	4.28	3.24
SHIP 2025A1B	4.99	4.39	4.55	3.90	4.70	4.12
SHIP 2050A1B	5.96	4.87	5.68	4.78	5.85	4.81
ROAD 2000	1.57	−0.141	1.74	1.50	1.76	2.21
ROAD 2025A1B	1.33	0.148	1.25	1.26	1.18	2.07
ROAD 2050A1B	0.332	0.210	0.302	0.314	0.282	0.548

Table A2. Radiative forcings ($mW\,m^{-2}$) from changes in ozone, methane (including stratospheric water vapour), and methane-induced ozone ($O_{3(CH_4)}$) for different transport sectors and years. Note that the history of emissions has been taken into account, and that the fully scaled perturbations were used.

	TM4				p-TOMCAT				OsloCTM2			
	O_3	CH_4	$O_{3(CH_4)}$	total	O_3	CH_4	$O_{3(CH_4)}$	total	O_3	CH_4	$O_{3(CH_4)}$	total
AIR 2025A1B	22.1	−17.7	−6.46	−2.06	48.4	−21.3	−7.77	19.4	24.6	−10.5	−3.82	10.3
AIR 2050A1B	52.1	−40.7	−14.9	−3.49	83.1	−40.8	−14.9	27.3	49.9	−23.9	−8.74	17.3
SHIP 2025A1B	26.6	−48.0	−17.5	−38.9	21.9	−42.2	−15.4	−35.6	40.6	−43.7	−16.0	−19.1
SHIP 2050A1B	36.0	−63.3	−23.1	−50.4	27.5	−51.8	−18.9	−43.2	55.2	−60.4	−22.1	−27.3
ROAD 2025A1B	19.8	−16.2	−5.90	−2.23	11.8	−1.80	−0.658	9.38	28.5	−15.2	−5.54	7.74
ROAD 2050A1B	6.46	−7.06	−2.58	−3.17	2.51	−4.46	−1.63	−3.58	8.60	−6.41	−2.34	−0.158
	LMDz-INCA				UCI CTM				MOCAGE			
	O_3	CH_4	$O_{3(CH_4)}$	total	O_3	CH_4	$O_{3(CH_4)}$	total	O_3	CH_4	$O_{3(CH_4)}$	total
AIR 2025A1B	20.8	−13.5	−4.91	2.43	30.9	−18.3	−6.69	5.83	34.3	−19.1	−6.96	8.31
AIR 2050A1B	46.4	−30.6	−11.2	4.67	67.0	−41.5	−15.1	10.4	69.3	−40.9	−14.9	13.5
SHIP 2025A1B	22.1	−37.5	−13.7	−29.1	39.4	−45.2	−16.5	−22.3	16.0	−39.6	−14.5	−38.1
SHIP 2050A1B	29.6	−50.8	−18.5	−39.7	53.2	−62.2	−22.7	−31.7	19.7	−51.1	−18.7	−50.1
ROAD 2025A1B	23.8	−15.3	−5.59	2.89	24.2	−14.3	−5.24	4.65	20.2	−25.1	−9.17	−14.0
ROAD 2050A1B	7.43	−6.68	−2.44	−1.69	7.48	−6.00	−2.19	−0.710	6.42	−11.7	−4.26	−9.49

Acknowledgements. This work was funded by the European Union's Sixth Framework Programme (FP6/2002-2006) through the QUANTIFY Integrated Project under contract no. 003893 (GOCE), and through the Network of Excellence ECATS (Project no. ANE4-CT-2005-012284). ØH has received funding from the Research Council of Norway through project no. 188134/E10 and the project TEMPO. GM has also received funding from the project TEMPO. Emission data sets were provided by the QUANTIFY partners MMU (aircraft), DNV (shipping), DLR (road traffic) and JRC (other anthropogenic emissions).

Edited by: R. Harley

References

Balkanski, Y., Myhre, G., Gauss, M., Rädel, G., Highwood, E. J., and Shine, K. P.: Direct radiative effect of aerosols emitted by transport: from road, shipping and aviation, Atmos. Chem. Phys., 10, 4477–4489, doi:10.5194/acp-10-4477-2010, 2010.

Berntsen, T. K., Myhre, G., Stordal, F., and Isaksen, I. S. A.: Time evolution of tropospheric ozone and its radiative forcing, J. Geophys. Res.-Atmos., 105, 8915–8930, doi:10.1029/1999jd901139, 2000.

Berntsen, T. K., Fuglestvedt, J. S., Joshi, M. M., Shine, K. P., Stuber, N., Ponater, M., Sausen, R., Hauglustaine, D. A., and Li,

L.: Response of climate to regional emissions of ozone precursors: sensitivities and warming potentials, Tellus B, 57, 283–304, 2005.

Borken, J., Steller, H., Meretei, T., and Vanhove, F.: Global and country inventory of road passenger and freight transportation - Fuel consumption and emissions of air pollutants in year 2000, Transp. Res. Record, 2011, 127–136, 10.3141/2011-14, 2007.

Burkhardt, U. and Karcher, B.: Global radiative forcing from contrail cirrus, Nat. Clim. Chang., 1, 54–58, doi:10.1038/nclimate1068, 2011.

Cariolle, D., Caro, D., Paoli, R., Hauglustaine, D. A., Cuenot, B., Cozic, A., and Paugam, R.: Parameterization of plume chemistry into large-scale atmospheric models: Application to aircraft NOx emissions, J. Geophys. Res.-Atmos., 114, D19302, doi:10.1029/2009jd011873, 2009.

Dahlmann, K., Grewe, V., Ponater, M., and Matthes, S.: Quantifying the contributions of individual NO(x) sources to the trend in ozone radiative forcing, Atmospheric Environment, 45, 2860–2868, doi:10.1016/j.atmosenv.2011.02.071, 2011.

Eide, M. S., Endresen, O., Mjelde, A., Mangset, L. E., and Gravir, G.: Ship emissions of the future. Technical Report No 2007-1325, Det Norske Veritas, Høvik, Norway, 1–98, 2007.

Endresen, O., Sorgard, E., Behrens, H. L., Brett, P. O., and Isaksen, I. S. A.: A historical reconstruction of ships' fuel consumption and emissions, J. Geophys. Res.-Atmos., 112, D12301, doi:10.1029/2006jd007630, 2007.

Eyring, V., Stevenson, D. S., Lauer, A., Dentener, F. J., Butler, T., Collins, W. J., Ellingsen, K., Gauss, M., Hauglustaine, D. A., Isaksen, I. S. A., Lawrence, M. G., Richter, A., Rodriguez, J. M., Sanderson, M., Strahan, S. E., Sudo, K., Szopa, S., van Noije, T. P. C., and Wild, O.: Multi-model simulations of the impact of international shipping on Atmospheric Chemistry and Climate in 2000 and 2030, Atmos. Chem. Phys., 7, 757–780, doi:10.5194/acp-7-757-2007, 2007.

Eyring, V., Isaksen, I. S. A., Berntsen, T., Collins, W. J., Corbett, J. J., Endresen, O., Grainger, R. G., Moldanova, J., Schlager, H., and Stevenson, D. S.: Transport impacts on atmosphere and climate: Shipping, Atmospheric Environment, 44, 4735–4771, doi:10.1016/j.atmosenv.2009.04.059, 2010.

Folberth, G. A., Hauglustaine, D. A., Lathière, J., and Brocheton, F.: Interactive chemistry in the Laboratoire de Météorologie Dynamique general circulation model: model description and impact analysis of biogenic hydrocarbons on tropospheric chemistry, Atmos. Chem. Phys., 6, 2273–2319, doi:10.5194/acp-6-2273-2006, 2006.

Franke, K., Eyring, V., Sander, R., Hendricks, J., Lauer, A., and Sausen, R.: Toward effective emissions of ships in global models, Meteorol. Z., 17, 117–129, doi:10.1127/0941-2948/2008/0277, 2008.

Fuglestvedt, J., Berntsen, T., Myhre, G., Rypdal, K., and Skeie, R. B.: Climate forcing from the transport sectors, Proc. Natl. Acad. Sci. USA, 105, 454–458, doi:10.1073/pnas.0702958104, 2008.

Gauss, M., Isaksen, I. S. A., Wong, S., and Wang, W. C.: Impact of H2O emissions from cryoplanes and kerosene aircraft on the atmosphere, J. Geophys. Res.-Atmos., 108, 4304, doi:10.1029/2002jd002623, 2003a.

Gauss, M., Myhre, G., Pitari, G., Prather, M. J., Isaksen, I. S. A., Berntsen, T. K., Brasseur, G. P., Dentener, F. J., Derwent, R. G., Hauglustaine, D. A., Horowitz, L. W., Jacob, D. J., Johnson, M., Law, K. S., Mickley, L. J., Muller, J. F., Plantevin, P. H., Pyle, J. A., Rogers, H. L., Stevenson, D. S., Sundet, J. K., van Weele, M., and Wild, O.: Radiative forcing in the 21st century due to ozone changes in the troposphere and the lower stratosphere, J. Geophys. Res.-Atmos., 108, 4292, doi:10.1029/2002jd002624, 2003b.

Granier, C. and Brasseur, G. P.: The impact of road traffic on global tropospheric ozone, Geophys. Res. Lett., 30, 1086, doi:10.1029/2002gl015972, 2003.

Grewe, V. and Stenke, A.: AirClim: an efficient tool for climate evaluation of aircraft technology, Atmos. Chem. Phys., 8, 4621–4639, doi:10.5194/acp-8-4621-2008, 2008.

Grewe, V., Dameris, M., Hein, R., Kohler, I., and Sausen, R.: Impact of future subsonic aircraft NOx emissions on the atmospheric composition, Geophys. Res. Lett., 26, 47–50, 1999.

Grewe, V., Tsati, E., and Hoor, P.: On the attribution of contributions of atmospheric trace gases to emissions in atmospheric model applications, Geosci. Model Dev., 3, 487–499, doi:10.5194/gmd-3-487-2010, 2010.

Grewe, V., Dahlmann, K., Matthes, S., and Steinbrecht, W.: Attributing ozone to NOx emissions: Implications for climate mitigation measures, Atmos. Environ., 59, 102–107, doi:10.1016/j.atmosenv.2012.05.002, 2012.

Grooß, J. U., Bruhl, C., and Peter, T.: Impact of aircraft emissions on tropospheric and stratospheric ozone. Part I: Chemistry and 2-D model results, Atmos. Environ., 32, 3173–3184, 1998.

Hauglustaine, D. A., Hourdin, F., Jourdain, L., Filiberti, M. A., Walters, S., Lamarque, J. F., and Holland, E. A.: Interactive chemistry in the Laboratoire de Meteorologie Dynamique general circulation model: Description and background tropospheric chemistry evaluation, J. Geophys. Res.-Atmos., 109, D04314, doi:10.1029/2003jd003957, 2004.

Hodnebrog, Ø., Berntsen, T. K., Dessens, O., Gauss, M., Grewe, V., Isaksen, I. S. A., Koffi, B., Myhre, G., Olivié, D., Prather, M. J., Pyle, J. A., Stordal, F., Szopa, S., Tang, Q., van Velthoven, P., Williams, J. E., and Ødemark, K.: Future impact of non-land based traffic emissions on atmospheric ozone and OH – an optimistic scenario and a possible mitigation strategy, Atmos. Chem. Phys., 11, 11293–11317, doi:10.5194/acp-11-11293-2011, 2011.

Holmes, C. D., Tang, Q., and Prather, M. J.: Uncertainties in climate assessment for the case of aviation NO, Proc. Natl. Acad. Sci. USA, 108, 10997–11002, doi:10.1073/pnas.1101458108, 2011.

Hoor, P., Borken-Kleefeld, J., Caro, D., Dessens, O., Endresen, O., Gauss, M., Grewe, V., Hauglustaine, D., Isaksen, I. S. A., Jöckel, P., Lelieveld, J., Myhre, G., Meijer, E., Olivie, D., Prather, M., Schnadt Poberaj, C., Shine, K. P., Staehelin, J., Tang, Q., van Aardenne, J., van Velthoven, P., and Sausen, R.: The impact of traffic emissions on atmospheric ozone and OH: results from QUANTIFY, Atmos. Chem. Phys., 9, 3113–3136, doi:10.5194/acp-9-3113-2009, 2009.

Hsu, J., Prather, M. J., and Wild, O.: Diagnosing the stratosphere-to-troposphere flux of ozone in a chemistry transport model, J. Geophys. Res.-Atmos., 110, D19305, doi:10.1029/2005jd006045, 2005.

Huszar, P., Cariolle, D., Paoli, R., Halenka, T., Belda, M., Schlager, H., Miksovsky, J., and Pisoft, P.: Modeling the regional impact of ship emissions on NO_x and ozone levels over the Eastern Atlantic and Western Europe using ship plume parameterization, Atmos. Chem. Phys., 10, 6645–6660, doi:10.5194/acp-10-6645-

2010, 2010.

IPCC: Climate Change 2001: The Scientific Basis. Contribution of Working Group I to the Third Assessment Report of the Intergovernmental Panel on Climate Change, edited by: Houghton, J.T., Ding, Y., Griggs, D.J., Noguer, M., van der Linden, P. J., Dai, X., Maskell, K., and Johnson, C. A., Cambridge University Press, Cambridge, United Kingdom and New York, NY, USA., 881 pp., 2001.

Jöckel, P., Tost, H., Pozzer, A., Brühl, C., Buchholz, J., Ganzeveld, L., Hoor, P., Kerkweg, A., Lawrence, M. G., Sander, R., Steil, B., Stiller, G., Tanarhte, M., Taraborrelli, D., van Aardenne, J., and Lelieveld, J.: The atmospheric chemistry general circulation model ECHAM5/MESSy1: consistent simulation of ozone from the surface to the mesosphere, Atmos. Chem. Phys., 6, 5067–5104, doi:10.5194/acp-6-5067-2006, 2006.

Koffi, B., Szopa, S., Cozic, A., Hauglustaine, D., and van Velthoven, P.: Present and future impact of aircraft, road traffic and shipping emissions on global tropospheric ozone, Atmos. Chem. Phys., 10, 11681–11705, doi:10.5194/acp-10-11681-2010, 2010.

Kraabøl, A. G., Berntsen, T. K., Sundet, J. K., and Stordal, F.: Impacts of NOx emissions from subsonic aircraft in a global three-dimensional chemistry transport model including plume processes, J. Geophys. Res.-Atmos., 107, 4655, doi:10.1029/2001jd001019, 2002.

Lee, D. S., Fahey, D. W., Forster, P. M., Newton, P. J., Wit, R. C. N., Lim, L. L., Owen, B., and Sausen, R.: Aviation and global climate change in the 21st century, Atmos. Environ., 43, 3520–3537, doi:10.1016/j.atmosenv.2009.04.024, 2009.

Lee, D. S., Pitari, G., Grewe, V., Gierens, K., Penner, J. E., Petzold, A., Prather, M. J., Schumann, U., Bais, A., Berntsen, T., Iachetti, D., Lim, L. L., and Sausen, R.: Transport impacts on atmosphere and climate: Aviation, Atmos. Environ., 44, 4678–4734, doi:10.1016/j.atmosenv.2009.06.005, 2010.

Matthes, S., Grewe, V., Sausen, R., and Roelofs, G.-J.: Global impact of road traffic emissions on tropospheric ozone, Atmos. Chem. Phys., 7, 1707–1718, doi:10.5194/acp-7-1707-2007, 2007.

Meijer, E. W., vanVelthoven, P. F. J., Wauben, W. M. F., Beck, J. P., and Velders, G. J. M.: The effects of the conversion of nitrogen oxides in aircraft exhaust plumes in global models, Geophys. Res. Lett., 24, 3013–3016, 1997.

Myhre, G., Karlsdottir, S., Isaksen, I. S. A., and Stordal, F.: Radiative forcing due to changes in tropospheric ozone in the period 1980 to 1996, J. Geophys. Res.-Atmos., 105, 28935–28942, 2000.

Myhre, G., Nilsen, J. S., Gulstad, L., Shine, K. P., Rognerud, B., and Isaksen, I. S. A.: Radiative forcing due to stratospheric water vapour from CH4 oxidation, Geophys. Res. Lett., 34, L01807, doi:10.1029/2006gl027472, 2007.

Myhre, G., Shine, K. P., Rädel, G., Gauss, M., Isaksen, I. S. A., Tang, Q., Prather, M. J., Williams, J. E., van Velthoven, P., Dessens, O., Koffi, B., Szopa, S., Hoor, P., Grewe, V., Borken-Kleefeld, J., Berntsen, T. K., and Fuglestvedt, J. S.: Radiative forcing due to changes in ozone and methane caused by the transport sector, Atmos. Environ., 45, 387–394, doi:10.1016/j.atmosenv.2010.10.001, 2011.

Nakicenovic, N., Davidson, O., Davis, G., Grübler, A., Kram, T., La Rovere, E. L., Metz, B., Morita, T., Pepper, W., Pitcher, H., Sankovski, A., Shukla, P., Swart, R., Watson, R., and Dadi, Z.: Special Report on Emissions Scenarios, Cambridge University Press, Cambridge, 599 pp., 2000.

Niemeier, U., Granier, C., Kornblueh, L., Walters, S., and Brasseur, G. P.: Global impact of road traffic on atmospheric chemical composition and on ozone climate forcing, J. Geophys. Res.-Atmos., 111, D09301, doi:10.1029/2005jd006407, 2006.

O'Connor, F. M., Carver, G. D., Savage, N. H., Pyle, J. A., Methven, J., Arnold, S. R., Dewey, K., and Kent, J.: Comparison and visualisation of high-resolution transport modelling with aircraft measurements, Atmos. Sci. Lett., 6, 164–170, doi:10.1002/asl.111, 2005.

Olivié, D. J. L., Cariolle, D., Teyssèdre, H., Salas, D., Voldoire, A., Clark, H., Saint-Martin, D., Michou, M., Karcher, F., Balkanski, Y., Gauss, M., Dessens, O., Koffi, B., and Sausen, R.: Modeling the climate impact of road transport, maritime shipping and aviation over the period 1860–2100 with an AOGCM, Atmos. Chem. Phys., 12, 1449–1480, doi:10.5194/acp-12-1449-2012, 2012.

Owen, B., Lee, D. S., and Lim, L.: Flying into the Future: Aviation Emissions Scenarios to 2050, Environ. Sci. Technol., 44, 2255–2260, doi:10.1021/es902530z, 2010.

Paoli, R., Cariolle, D., and Sausen, R.: Review of effective emissions modeling and computation, Geosci. Model Dev., 4, 643-667, doi:10.5194/gmd-4-643-2011, 2011.

Peters, G. P., Marland, G., Le Quere, C., Boden, T., Canadell, J. G., and Raupach, M. R.: Rapid growth in CO2 emissions after the 2008-2009 global financial crisis, Nat. Clim. Chang., 2, 2–4, 2012.

Schnadt Poberaj, C., Staehelin, J., Bintania, R., van Velthoven, P., Dessens, O., Gauss, M., Isaksen, I. S. A., Grewe, V., Jöckel, P., Hoor, P., Koffi, B., Hauglustaine, D., and Olivié, D.: QUANTIFY model evaluation of global chemistry models: carbon monoxide, Proceedings of the 2nd International Conference on Transport, Atmosphere and Climate, Aachen, Germany, 22–25 June 2009, DLR Forschungsbericht 2010-10, ISSN 1434-8454,163-168, 2010,

Skeie, R. B., Fuglestvedt, J., Berntsen, T., Lund, M. T., Myhre, G., and Rypdal, K.: Global temperature change from the transport sectors: Historical development and future scenarios, Atmos. Environ., 43, 6260–6270, doi:10.1016/j.atmosenv.2009.05.025, 2009.

Søvde, O. A., Gauss, M., Smyshlyaev, S. P., and Isaksen, I. S. A.: Evaluation of the chemical transport model Oslo CTM2 with focus on arctic winter ozone depletion, J. Geophys. Res.-Atmos., 113, D09304, doi:10.1029/2007jd009240, 2008.

Teyssèdre, H., Michou, M., Clark, H. L., Josse, B., Karcher, F., Olivié, D., Peuch, V.-H., Saint-Martin, D., Cariolle, D., Attié, J.-L., Nédélec, P., Ricaud, P., Thouret, V., van der A, R. J., Volz-Thomas, A., and Chéroux, F.: A new tropospheric and stratospheric Chemistry and Transport Model MOCAGE-Climat for multi-year studies: evaluation of the present-day climatology and sensitivity to surface processes, Atmos. Chem. Phys., 7, 5815–5860, doi:10.5194/acp-7-5815-2007, 2007.

Uherek, E., Halenka, T., Borken-Kleefeld, J., Balkanski, Y., Berntsen, T., Borrego, C., Gauss, M., Hoor, P., Juda-Rezler, K., Lelieveld, J., Melas, D., Rypdal, K., and Schmid, S.: Transport impacts on atmosphere and climate: Land transport, Atmos. Environ., 44, 4772–4816, doi:10.1016/j.atmosenv.2010.01.002, 2010.

Unger, N., Shindell, D. T., Koch, D. M., and Streets, D. G.: Air pollution radiative forcing from specific emissions sectors at 2030, J. Geophys. Res., 113, D02306, doi:10.1029/2007jd008683, 2008.

van Aardenne, J. A., Dentener, F. D., Olivier, J. G. J., Peters, J. A. H. W., and Ganzeveld, L. N.: The EDGAR 3.2 Fast Track 2000 dataset (32FT2000), http://themasites.pbl.nl/tridion/en/themasites/edgar/emission_data/edgar_32ft2000/documentation/index-2.html, Joint Research Center, Institute for Environment and Sustainability (JRC-IES), Climate Change Unit, Ispra, Italy, 2005.

van der Werf, G. R., Randerson, J. T., Giglio, L., Collatz, G. J., Kasibhatla, P. S., and Arellano Jr., A. F.: Interannual variability in global biomass burning emissions from 1997 to 2004, Atmos. Chem. Phys., 6, 3423–3441, doi:10.5194/acp-6-3423-2006, 2006.

Vinken, G. C. M., Boersma, K. F., Jacob, D. J., and Meijer, E. W.: Accounting for non-linear chemistry of ship plumes in the GEOS-Chem global chemistry transport model, Atmos. Chem. Phys., 11, 11707–11722, doi:10.5194/acp-11-11707-2011, 2011.

Wild, O. and Prather, M. J.: Excitation of the primary tropospheric chemical mode in a global three-dimensional model, J. Geophys. Res.-Atmos., 105, 24647–24660, doi:10.1029/2000jd900399, 2000.

Wild, O., Prather, M. J., and Akimoto, H.: Indirect long-term global radiative cooling from NO_x emissions, Geophys. Res. Lett., 28, 1719–1722, doi:10.1029/2000gl012573, 2001.

Wild, O., Sundet, J. K., Prather, M. J., Isaksen, I. S. A., Akimoto, H., Browell, E. V., and Oltmans, S. J.: Chemical transport model ozone simulations for spring 2001 over the western Pacific: Comparisons with TRACE-P lidar, ozonesondes, and Total Ozone Mapping Spectrometer columns, J. Geophys. Res.-Atmos., 108, 8826, doi:10.1029/2002jd003283, 2003.

Williams, J. E., Scheele, M. P., van Velthoven, P. F. J., Thouret, V., Saunois, M., Reeves, C. E., and Cammas, J.-P.: The influence of biomass burning and transport on tropospheric composition over the tropical Atlantic Ocean and Equatorial Africa during the West African monsoon in 2006, Atmos. Chem. Phys., 10, 9797–9817, doi:10.5194/acp-10-9797-2010, 2010.